JOURNAL GEOLOGICAL SOCIETY OF INDIA
Vol.92, August 2018, pp.201-208

Paleoweathering and Paleoclimatic Reconstructions using Neoproterozoic Paleosol in the Eastern Margin of the Pranhita-Godavari Basin, India

Vijay Sharma[1], Pitambar Pati[1*], M. L. Dora[2], Narendra K. Patel[1], Chinmay Dash[1], Parvej Alam[1], Aditya K. Verma[1], Ankit Gupta[1]

[1] Indian Institute of Technology Roorkee, Roorkee - 247 667, India
[2] Geological Survey of India, Central Region, Nagpur - 440 006, India
***E-mail:** impitambarpati@gmail.com*

ABSTRACT

A thin, weakly-developed palaeosol horizon within the Neoproterozoic Sullavai sandstone in the eastern margin of the Pranhita-Godavari basin was studied. Field observations, thin-section studies and geochemical analyses of the palaeosol horizon were carried out to reconstruct the palaeo-weathering and palaeoclimatic conditions. The palaeosol developed on sandstone parent rock. Morphological features of this palaeosol are not distinct, perhaps due to very ancient nature as well as thin occurrence. A few of which that can be mentioned include weakly developed peds and calcareous nodules of size <1 cm - .2 cm. The lower part of the profile preserves incipient parent rocklamination. Major micromorphological features of this palaeosol include weakly-developed sub-angular blocky structure and redoximorphic features showing redox enrichment and redox depletion of Fe oxides and oxyhydroxides. XRD analysis of the palaeosol reveals the presence of glauconite and illite, suggesting deposition of sediments under shallow marine conditions, and prevalence of cold climate, respectively. This is also supported from Chemical Index of Alteration (CIA)and presence of illite. Further, Chemical Index of Weathering (CIW), Clayeness, and Salinization data of the palaeosol clearly suggests an environment where chemical weathering was feeble and cold (11-14°C) palaeo-temperature. XRF results show abundance of K, Ca and Mg which suggest the area was poorly drained along with cooler palaeoclimate during the late Neoproterozoic. Al_2O_3 concentration at the middle of the soil profile suggests weakly-developed B-horizon, however it is hardly observed in the field. Parent material, cold climate and less time of exposure only resulted in the formation of a thin and weakly-developed soil profile. This ancient soil may represent an unconformity at the basin boundary suggesting a local regression and exposure of the fluvio-marine deposits along the basin boundary. It further needs detailed such studies at various spatio-temporal basinal scales.

INTRODUCTION

Palaeosols, ranging from Precambrian to Recent, are increasingly recognized for a wide number of geological applications, particularly for palaeoclimate, palaeolandscape and tectonic as well as neotectonic reconstructions (Holland, 1994; Kraus, 1999; Retallack, 2001, 2013; Sheldon, 2006; Sheldon and Tabor, 2009; Bhargava et al., 2011; Pati et al., 2012; Singh et al., 2013; Driese and Nordt, 2013; Mukhopadhyay et al., 2014; Singh et al., 2015, 2017 and many more).These are also used as tools for addressing the Precambrian atmospheric composition, as they form by direct interaction with the atmosphere (Holland, 1984; Retallack et al., 1984; Retallack, 2013).

Also these have been discovered and documented in large numbers from different geological environments i.e. continental depositional settings including eolian (Soreghan et al., 1997), palustrine (Tandon et al., 1995;Wright and Platt, 1995;Tandon and Gibling, 1997), deltaic sequences (Fastovsky and McSweeney, 1987; Arndorff, 1993),marginal marine (Lander et al., 1991; Wright, 1994),and in marine sediments (Driese et al., 1994; Webb, 1994). Palaeosol presence represents a hiatus in the stratigraphy and has regional significance in the geological history of the area (Bhargava et al., 2011).

Study of palaeosol is a field science (Retallack, 1988) and hence, its recognition and properties like soil-horizons and structures are best studied in the field (Retallack, 1992). But, in the areas of deformation and metamorphism subsequent to the formation of weathering profile such as those found in many Precambrian terrains, field recognition and their morphological features become cumbersome. Therefore, quantitative and micromorphological studies of palaeosols are widely used worldwide for a number of investigations including differentiating between metasomatic alteration of sedimentary rocks and pedogenesis (Retallack, 1986; Zbinden et al., 1988; Holland et al., 1989; Maynard., 1992; Sheldon, 2006) as well as determining palaeo-temperature and weathering patterns.

The Pranhita-Godavari basin (Fig. 1) was formed in the mid-northern latitude (Torswik et al., 2001; Gregory et al., 2009; Valdiya, 2010) during the existence of the Rodinia Supercontinent. This fossil rift shows several extensional episodes witnessed by igneous activities along the basin boundary (Dora and Randive, 2015) and shift of shorelines at different intervals (Ghosh and Saha, 2003). Due to extensional tectonics, the basin boundary shows faulted margin and the facies association at the boundary zone suggests the sediment accumulation in narrow, relatively shallow and isolated sub-basins separated by horsts and grabens(Fig. 2), and evolved through fairly deep continental sea through time (Deb, 2003).

Though a number of research papers have been published in the last decade highlighting the depositional environment and tectonism of the Pranhita-Godavari basin, most of those are confined along the western margin. In addition, studies on palaeoclimatic regime during the deposition are lacking. The present study attempts to bridge this gap by using the palaeosol geochemisty as a tool to decipher the palaeoweathering and palaeoclimatic regime of the basin margin during the palaeosol formation. Palaeosol shows periods of stable landscape following unconformities, if found solitary (Krauss, 1999). Sedimentation and erosion rates due to various autogenic and allogenic processes within the basin decides thickness of palaeosol and degree of pedogenesis (e.g., Himalayan Foreland Basin; Singh et al., 2015; 2017). Regionally, palaeosol helps in stratigraphic correlations across regions like Pakistan to Nepal in Himalayas (Singh et al., 2017) as

0016-7622/2018-92-2-201/$ 1.00 © GEOL. SOC. INDIA | DOI: 10.1007/s12594-018-0982-y

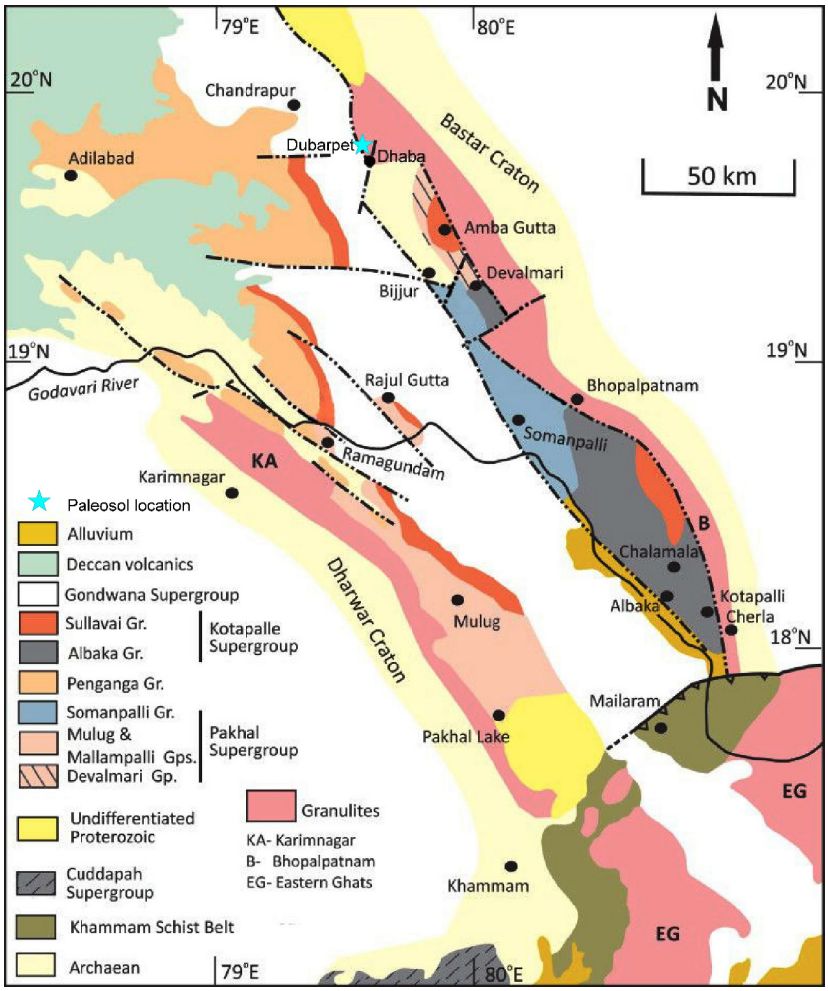

Fig.1. Regional map of the Pranhita-Godavari basin (after Amarasinghe et al., 2015). The palaeosol location is marked as a star

well as palaeoprecipitation studies, palaeo-temperature studies, palaeoclimatic reconstructions or documentation of pre-Archaean great oxygenation events (Mukhopadhyay et al., 2014). Globally, models of palaeosol climofunction studies using mean annual temperature or mean annual precipitation, micromorphological and clay morphology analyses, seasonability are constructed for first interhemispheric global climate comparisons (Varela et al., 2017).

STUDY AREA

The Pranhita-Godavari basin is bounded by the Bastar craton in the east, the Dharwar craton in the west, the Deccan volcanic province in the northwest and the Eastern Ghat in the southeast(Fig. 1). Proterozoic sedimentary rocks in the basin occur as two NW-SE trending linear belts flanked by two belts of Archaean gneiss and granulite rocks along their outer margins and intervened by the Gondwana rocks in the middle (Chaudhuri et al., 2002).The present study area falls in the eastern margin of the basin, bounded by the latitudes 19°40'25" and 19°40'37"N and longitudes 79°39'09" and 79°39'17"E. The litho-association of the area ranges in age from lower Neoproterozoic to upper Neoproterozoic (Chaudhuri and Howard, 1985) and the Sullavai Group in particular, wherein the palaeosol is identified, yields the K-Ar age of 871±14 Ma (Chaudhuri and Howard, 1985). Stratigraphy of the area is given in Table 1. The westward dipping litho-package of the region represents a fan-delta deposit at the basin boundary consisting of conglomerate, sandstone (hosting the palaeosol) and shale (Fig. 3a). This lithopackage is overlain by a transgressive sequence consisting of sandstone and conglomerate at the basin margin, and limestone in the shelf environment (Fig. 2). Faulting induced block tilting has modified the primary depositional attitude of the litho package (Deb, 2003; Pati, 2010). Influence of faulting is well represented by intense silicification and chloritization of the rocks along the fault zone and autoclastic conglomerate in the basin-margin limestone sequence.

METHODOLOGY

The methodology adopted in the present study has been divided into four sections: field mapping of facies association and recognition of palaeosol, thin-section studies,XRD analysis and major element geochemistry of the palaeosol.

Field Mapping and Recognition of Palaeosol

Large scale field mapping (1:1000 scales) was carried out (Fig. 4) to map the facies association. Most parts of the litho-package along the basin margin are buried under recent sediments and soil; however, vertical sections are exposed in the sandstone queries (Fig. 3). The palaeosol horizon is developed on the top of quartz arenite (Fig. 3) and is overlain by a transgressive sequence consisting of sandstone and conglomerate. Though the average thickness of the soil profile is about 15 cm, but there are certain funnel-like extensions of more than the average thickness, probably representing extension of the weathering profile into the parent rock (Fig. 3a). The palaeosol development defines a time break in deposition at the marginal zone and a corresponding unconformity surface to certain extent into the basin interior (Fig. 2).

Palaeosols are difficult to recognize in early Paleozoic and Precambrian alluvial sedimentary rocks because they lack the large root traces of vascular plants that characterize late Paleozoic and geologically younger palaeosols (Retallack, 2001). Therefore, other field/ morphological and macroscopic characteristics such as colour, development of soil structures and nodules have been used for field recognition. Also, thickness and colour of different palaeosol horizons found, are documented in the field.

Table 1. Stratigraphy of the region (after Crookshank, 1963; Chaudhuri and Howard, 1985)

Gondwana Rocks
~ ~ ~ ~ ~ ~ ~ ~ ~ ~ ~ ~ ~ ~ unconformity ~ ~ ~ ~ ~ ~ ~ ~ ~ ~ ~ ~ ~ ~
Venkatpur Sandstone
Sullavai Group
Mancheral Quartzite
~ ~ ~ ~ ~ ~ ~ ~ ~ ~ ~ ~ ~ ~ unconformity ~ ~ ~ ~ ~ ~ ~ ~ ~ ~ ~ ~ ~ ~
Penganga/Pakhal Group
Abujhmar Group
~~unconformity~~~~~~~~~~~~~~~~~~~~~~~~
Dongargarh Supergroup
Sonakhan Schist Belt
~~unconformity~~~~~~~~~~~~~~~~~~~~~~~~
Bailadila
~~unconformity~~~~~~~~~~~~~~~~~~~~~~~~
Bengpal Group
~~unconformity~~~~~~~~~~~~~~~~~~~~~~~~
Sukma Group/TTG/Gneisses/granites

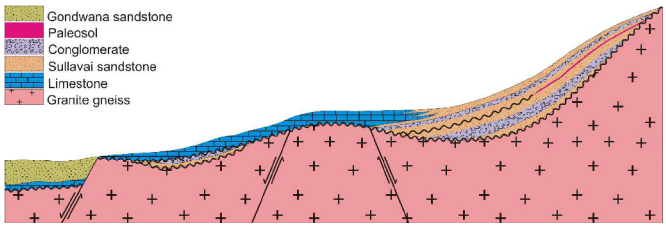

Fig.2. Model (schematic) showing development of palaeosol and unconformity in the basin, prepared based on field evidences and literature reviews.

Generally, various soil forming processes can be explained based on the presence (or absence) of well developed horizons preserved within strata (Birkeland, 1999; Buol et al., 1997). Even poorly developed palaeosols and their horizon characteristics elucidate the environment of soil formation. Sampling of palaeosol was carried out following Retallack, (1988). As the palaeosol horizon was extremely friable; samples were collected carefully in tin boxes for the preparation of thin sections. Bulk sampling of fresh-palaeosol was carried out by removing the upper surface from the exposure for geochemical study.

Thin-section Studies

As the palaeosol was very much friable, samples were soaked and hardened using a mixture of toluene and canada balsam as suggested by Liivamagi et al. (2015) and then cutting and polishing was carried out using slab saw and grinder for thin section preparation.

XRD Analysis

The palaeosol samples were grounded to a fine powder of ~200 mesh size. Powdered sample was spread uniformly over glass surface when monochromatic X-ray strikes the mount and diffracted in all possible directions as suggested by Klein and Dutrow (2008). The particles are oriented in such a way that they make a proper angle with incident beam to satisfy Bragg's Law. For each sample, one gram powder of palaeosol was analysed in single crystal X-ray diffractometer (SC-XRD) using K780 X-ray generator with Cu (Kα) as target. XRD analysis of palaeosol samples was carried out in the Burker D8 X-Ray diffrectometer (X-Ray source: 2.2kW Cu anode, 40 kV/40 mA, Detector: LINXEYE XE, angular range (2Theta): 5º to 120º, smallest angular step size: 0.0001º) in the Institute Instrumentation Centre, IIT Roorkee, India.

Major Element Geochemistry of the Palaeosol and its Application

Different proxies (Table 2) derived from the major element geochemistry have successfully been used for palaeo-environmental reconstruction (Liivamägi et al., 2015; Feakes and Retallack, 1988; Retallack, 1997; Sheldon et al., 2002; Sheldon, 2006; Sheldon and Tabor, 2009; Nordt and Driese, 2012). Bulk-sample geochemistry of palaeosol was determined through X-ray fluorescence spectroscopy (XRF).Three samples collected at 5 cm interval of the soil profile (PS-1/1, PS-1/2 and PS-1/3,Table 3) and other three bulk-samples (PS-2, PS-3 and PS-4) collected from different locations were analysed through XRF. Selected rock samples were powdered to less than 200 mess size by Jaw Crusher (Retsch BB 50) and Vibrating Disc Mill (Retsch RS 200) at Ore Geology and Fluid Inclusions Laboratory, Department of Earth Sciences, IIT Roorkee. Approximately 5 gm of powder from each sample was taken for preparing pressed pallets and analysed by Bruker S4 Poinner X-ray Spectrometer with end Window Rh X-ray Tube, 75 µm Be window in the Institute Instrumentation Center, IIT Roorkee, India.

Chemical Index of Weathering (CIW)

The chemical index of alteration (CIA; Nesbitt and Young, 1982) evaluates the degree of chemical weathering. CIA is a dimensionless

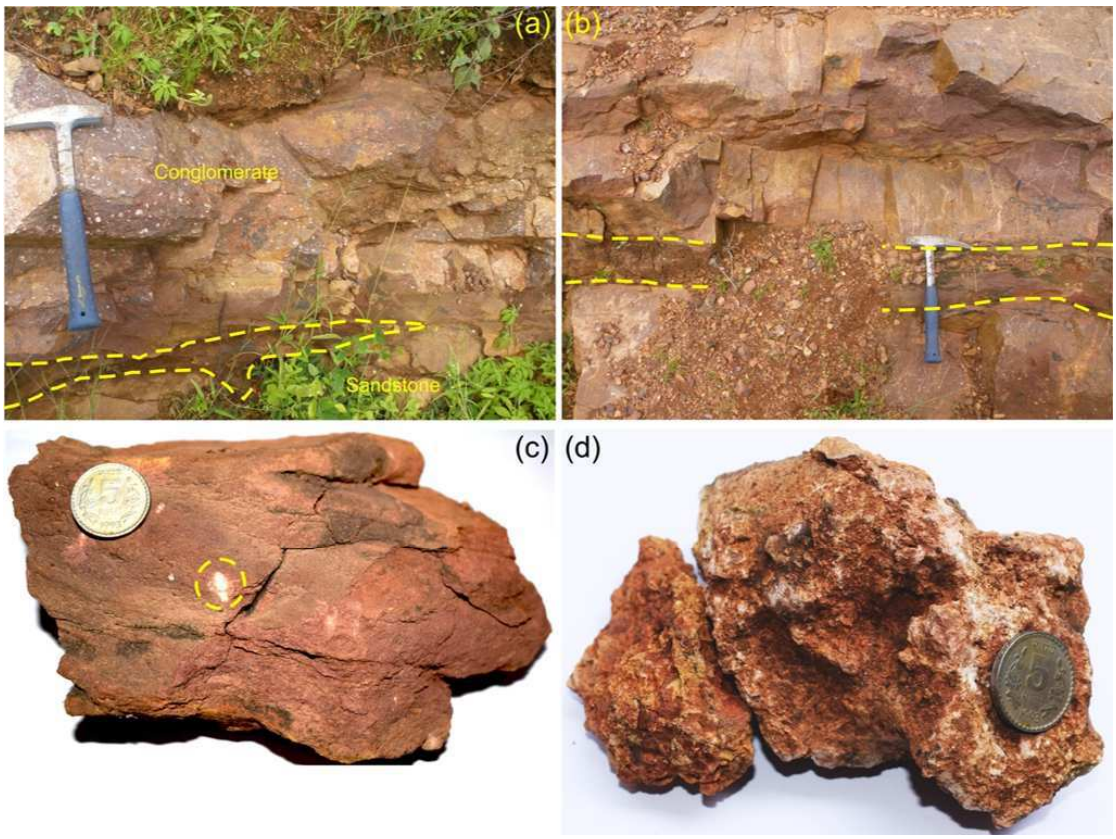

Fig.3. (a, b) Field photograph showing the palaeosol horizon and the overlying and underlying litho units, **(c)** occurrence of calcareous nodule in the soil and faintly developed sub-angular blocky structure, **(d)** Nodules recovered from fractures in the palaeosol.

Table 2. Proxies used for chemical analysis and their outcome (Sheldon and Tabor, 2009)

S. No.	Method	Outcome
1.	Major element weathering indices:	These index values represent extent of weathering.
	1) Chemical Index of Alteration (Al_2O_3/(Al_2O_3+Na_2O+K_2O+CaO)	Breakdown of Feldspars to clay.
	2) Chemical Index of Weathering (Al_2O_3/(Al_2O_3+Na_2O+CaO)K	Degree of weathering without
	3) Salinization (Na_2O+K_2O/Al_2O_3)	More salts accumulate during weathering.
	4) Clayeyness (Al_2O_3/SiO_2)	More clay production as rock weathers.
2.	Clay Mineralogy: Identification of clay minerals using the value of d-spacing, (XRD).	The type of clay mineral present will itself tell us climate.
3.	Paleotemperature T (°C) = -18.5S+17.3, where S is Salinization	High salinization value indicates low mean annual temperature (MAT)

number between 0 and 100 and shows the weathering of feldspar minerals and their hydration to clay minerals. It is calculated using molecular proportions:

$$CIA = [Al_2O_3/ (Al_2O_3 + CaO + Na_2O + K_2O)] \times 100$$

The CIA values do not change during metamorphism (Nesbitt and Young, 1982).The general understanding of this index lies in the assumption that as clay content increases in the upper part of the palaeosol profiles, Al should also increase and Ca, Na, K should decrease and this would lead to higher CIA values (Table 4). Although CIA is widely used, it does not account for the post-burial addition of K by metasomatism (Driese et al., 2007) or possible illitization of pedogenic clay minerals (e.g. smectite). Therefore, recently few authors (Maynard, 1992; Fedo et al., 1995) concerned about post burial addition of K by metasomatism. Also, due to addition of K, illitization of clay minerals (e.g. smectites) takes place in sub-metamorphic burial conditions. This is particularly important for Paleozoic and older palaeosols because smectite is meta-stable and may be altered to illite in the presence of K-rich pore waters. They introduced the term CIW (chemical index of weathering) and basic purpose behind was about the inconsistent behaviour of K during pedogenesis (Sheldon and Tabor, 2009).

$$CIW = [Al_2O_3/ (Al_2O_3+CaO+Na_2O)]\times100$$

The value of this index increases as the degree of weathering increases (Harnois, 1988).

Clayeyness

Clayeyness is the measure of clay content in the soil/palaeosol (Sheldon and Tabor, 2009; Ruxton, 1968). Cations such as Na^+, K^+, Ca^{2+}, and Si^{4+} are lost during chemical weathering. Al/Si is thought to be a measure of "clayeness" because Al accumulates in clay minerals relative to a silicate mineral. The ratio was first proposed (though inverted from the present form) by Ruxton (1968) and has been widely applied (Sheldon and Tabor, 2009; Retallack, 2000; Prochnow et al., 2006; Sheldon, 2006; Hamer et al., 2007).

$$Clayeness = Al_2O_3/SiO_2$$

The molar ratio of Al to Si is a function of the clayeyness of a palaeosol (Retallack, 1997).

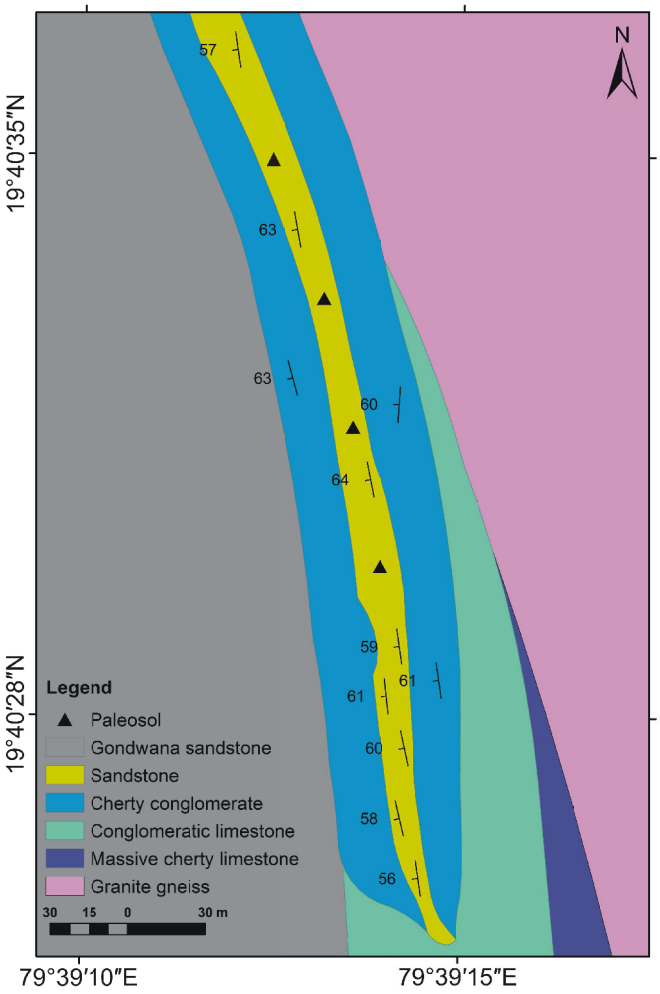

Fig.4. Large scale facies map of the study area around the palaeosol location

Salinization and Palaeo-temperature

Salinization is the process by which mobile cations such as K and Na (alkali elements) accumulate as soluble salts in soil or palaeosol where older examples are much more rare because salts are often removed by diagenesis, leaving evaporite mineral pseudomorphs rather

Table 3. Oxide weight percentage obtained from XRF

Oxides Sample	Na_2O wt%	MgO wt%	Al_2O_3 wt%	SiO_2 wt%	P_2O_5 wt%	SO_3 wt%	K_2O wt%	CaO wt%	TiO_2 wt%	V_2O_5 wt%	Cr_2O_3 wt%	MnO wt%	Fe_2O_3 wt%	CoO wt%	NiO wt%	CuO wt%	ZnO wt%	Rb_2O wt%	SrO wt%	ZrO_2 wt%
PS-1/1	0.00	1.25	13.18	61.38	0.11	0.00	2.80	0.09	0.48	0.00	0.05	0.02	5.13	0.01	0.00	0.12	0.00	0.01	0.00	0.03
PS-1/2	0.00	1.57	8.66	67.35	0.07	0.00	1.42	0.10	0.30	0.00	0.03	0.00	4.23	0.01	0.01	0.18	0.00	0.00	0.00	0.03
PS-1/3	0.00	1.07	8.48	70.64	0.07	0.00	1.60	0.08	0.33	0.00	0.02	0.03	4.02	0.02	0.01	0.14	0.00	0.01	0.00	0.03
PS-2	0.00	3.82	19.70	39.90	0.09	0.00	5.23	0.46	0.86	0.02	0.05	0.08	9.91	0.00	0.03	0.49	0.01	0.02	0.00	0.03
PS-3	0.00	2.73	24.40	45.10	0.05	0.00	7.15	0.14	0.89	0.02	0.03	0.07	7.54	0.02	0.01	0.43	0.01	0.03	0.00	0.04
PS-4	0.06	3.52	19.92	40.61	0.11	0.00	4.92	0.45	0.93	0.02	0.05	0.10	10.60	0.02	0.03	0.54	0.01	0.02	0.00	0.05
																			0.00	0.04

Table 4. CIA value and representing mineral (Nesbitt and Young, 1982; Fedo et al., 1995)

CIA Value	Mineral present
100	Kaolinite
75-90	Illite
75	Muscovite
50	Feldspar
30-45	Fresh basalts
45-55	Fresh granites and Granodiorites

than the original minerals (Sheldon and Tabor, 2009). A relation between palaeo-temperature and salinization was established by Sheldon et al. (2002) as:

$$T\ (°C) = -18.5S + 17.3,$$

where S is salinization and standard error RE = ± 4.4°C, R^2= 0.37, the temperature range for the formula is 2°-20°C (Sheldon et al., 2002).

$$\text{Salinization, } S = (Na_2O + K_2O)/Al_2O_3$$

It helps in finding the palaeo-temperature estimates which is a good proxy for finding the palaeoclimatic conditions.

RESULTS AND DISCUSSION

The studied palaeosol horizon is of ~15 cm thick, weakly developed and formed on the basin-margin sandstone (quartz arenite). The sandstone hosting the palaeosol is fairly mature consisting of more detrital quartz grains of polycrystalline nature (Fig. 5a). The quartz grains are derived from a metamorphic source (juxtaposed Archean basement) as evidenced by combination of more than five individual crystals or polycrystalline quartz present in a single grain (Boggs, 2006). The roundness of grains, its matrix content, cementation, dominance of quartz with the low amount of plagioclase/alkali feldspar (Fig. 5) brings it to fairly mature category as described by Prothero and Schwab (2004). Two samples from the same sandstone horizon shows different degree of angularity i.e. the oceanward part shows higher degree of roundness and less matrix (Fig. 5a) and the continent ward shows relatively less degree of roundness and more matrix content (Fig. 5b) which indicates continent ward fluvial influence. The upward coarsening nature of the formation can be interpreted as a fairly gradual shallowing sequence, with adjacent association of fluviatile environment. This litho-assamblege suggests a fan delta with exposed marine assembly (Johnson, 1975).

The identified thin, friable palaeosol lacks distinct morphological features. Nevertheless, weakly developed sub-angular blocky structure and presence of pedogenic carbonate nodules can be easily observed (Fig.3). The nodule size varies from 1 cm to > 2 cm. Soil colour varies from 5Y 7/4, 5Y7/3 and 7.5YR 5/8 which was noted using the Munsell soil colour chart (Munsell, 2005).

Photomicrographs of the upper part (1-5 cm) of the palaeosol horizon shows some weakly-developed pedo features such as sub-angular blocky structures and redoximorphic features showing redox enrichment and redox depletion of Fe oxides and oxyhydroxides (Fig. 6a, b) whereas, the lower part of the profile, crude laminations are preserved (Fig. 6c). Silica and iron encrustations on the grain boundary are seen in the lower part of the soil profile (Fig. 6d).

The minerals identified from XRD analyses (Fig. 7) are quartz, illite, glauconite and muscovite. Illite polytypes were determined using JCPDS (details given in Appendix-1).Clay minerals formed by weathering of all kind of silicates shows different climate and environment (Galan, 2006). Glauconite is a strong tool for reconstruction of palaeo-environment (Amorosi, 1997). It has dioctahedral (2:1) structure (Weaver, 1968) and its presence reveals the climate to be dominantly marine and within shallow water environment with slow and intermittent rates of deposition (Prothero and Schwab, 2004). It is one of the abundant mineral at unconformities; e.g., at the top of marine regressive sequences on which the palaeosol was developed. It is formed in reducing environment and normal shallow marine waters with depth ranging from 50 m to 500 m (Odin and Fullagar, 1988; McRae, 1972) as generally common in a fan-delta setting which fits to the present observation. To form, glauconite must reside at sediment-water interface for 1000 to 10,000 years (Odin and Matter, 1981). Illite, montmorillonite, and mixed layer illite-montmorillonite can occur in any major depositional environments (Weaver, 1956). Illite is the predominant clay mineral in the older Paleozoic clastic sediments and its abundance apparently is a reflection of source material and type of weathering rather than environmental diagenesis. The only significant source of 2M illites is muscovite and it appears that most of the illite in sediments was derived from muscovite and is therefore detrital in origin. In the present study, both illite and muscovite are present as seen from the XRD study, which may substantiate the claim.

CIA (Chemical Index of Alteration) values suggest the weathering trends in the palaeosols and ancient mudstones (Sheldon, 2003; Young et al., 1998). In the present study, CIA values for four palaeosol samples (Table-5) ranges from 75 to 83 which represent the presence of illite (Nesbitt and Young, 1982) which is also confirmed by the XRD peaks. There is decrease of CIA value at the top of the profile (0-5 cm) and slight increase in the middle (5-10 cm depth) indicating leaching of Al_2O_3 from the top and accumulation in the middle as generally is the

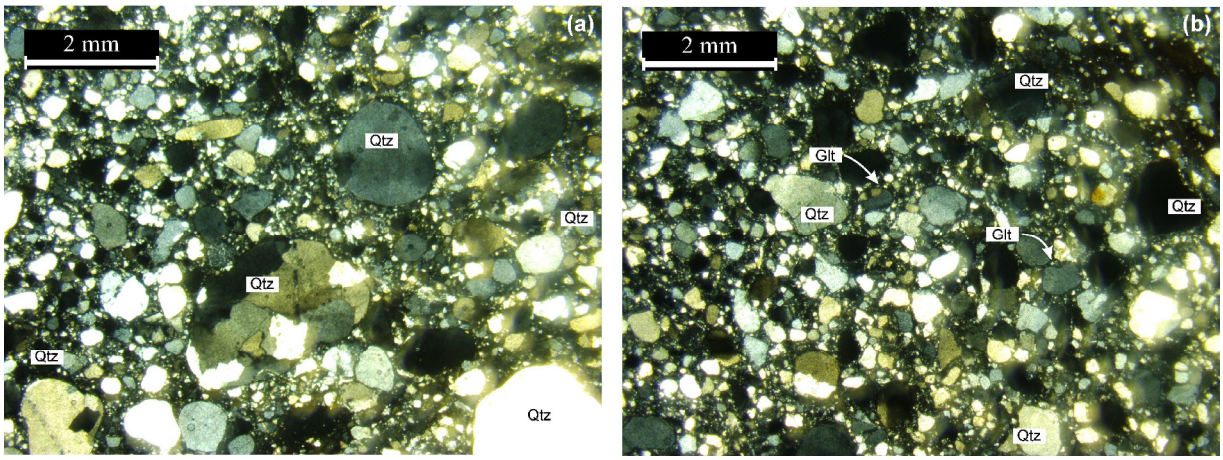

Fig.5. Thin-section showing presence of polycrystalline quartz in **(a)** and presence of glauconite in **(b).** The degree of grain angularity and matrix content vary from oceanward (a) to continentward (b) of the sandstone horizon. Qtz-Quartz, Glt- Glauconite

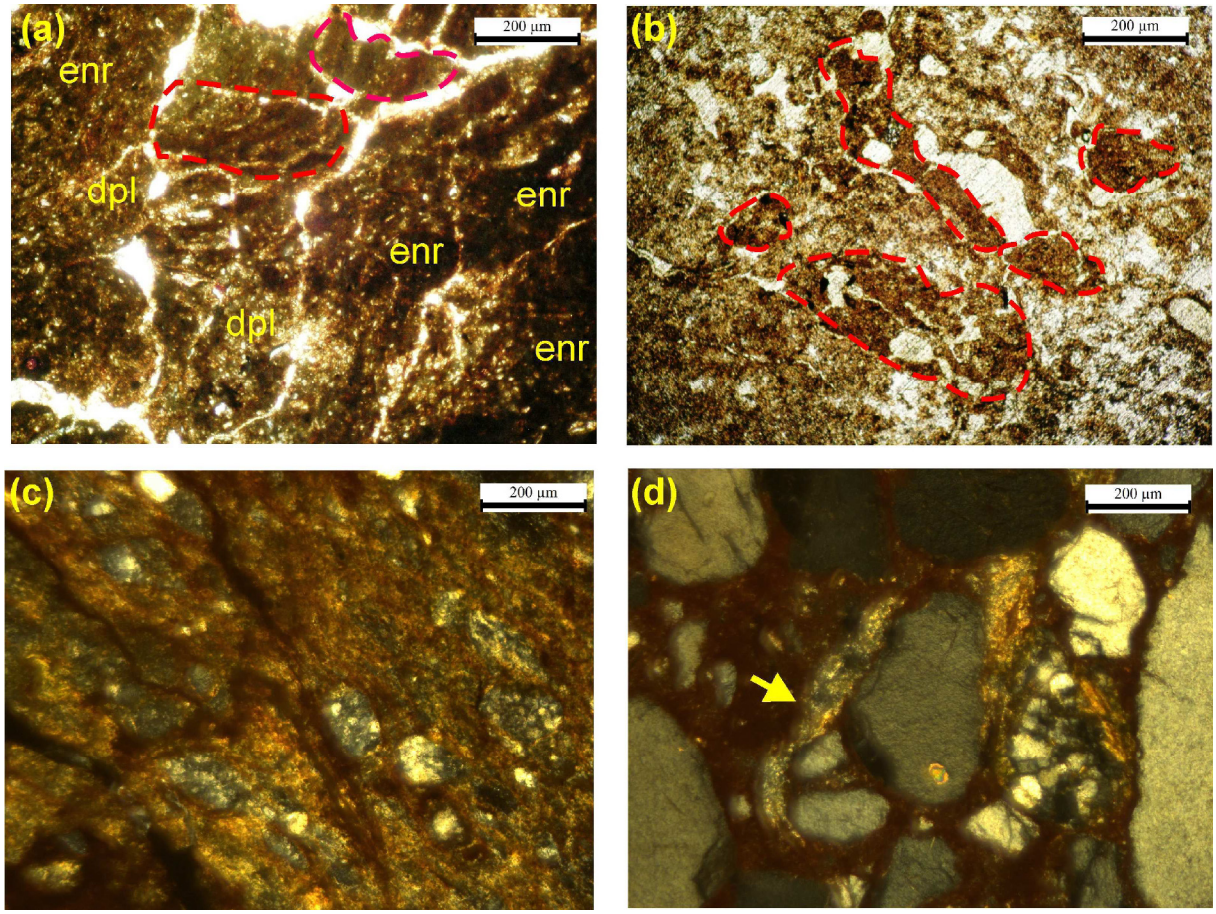

Fig.6. Thin-section of palaeosol (**a and b**) show development of subangular blocky structuresand ribbon-like structure (marked as red dotted lines),redoximorphic features showing redox enrichment (enr) and redox depletion (dpl) of Fe oxides and oxyhydroxides **(c)** shows crude lamination in the lower part of the soil horizon, **(d)** encrustation around the guartz grain and rock fragments as diagenetic changes.

case in soil profiles. CIW can be applied to both, modern and Precambrian soils. In the present case, the value of this index increases as the degree of weathering increases (Harnois, 1988). CIW values vary from 95-99 indicating higher degree of weathering.

Clayeyness of 0.07 to 0.3 (Table 5) indicates less Al_2O_3 concentration in the soil profile. As the weathering progresses, more clay is formed from degradation of feldspars. Hence, the ratio of Al_2O_3 to SiO_2 increases. The presently obtained value indicates feeble chemical weathering (clay formation) than physical weathering (Nesbitt and Young, 1982), which suggests the prevalence of cold climate.

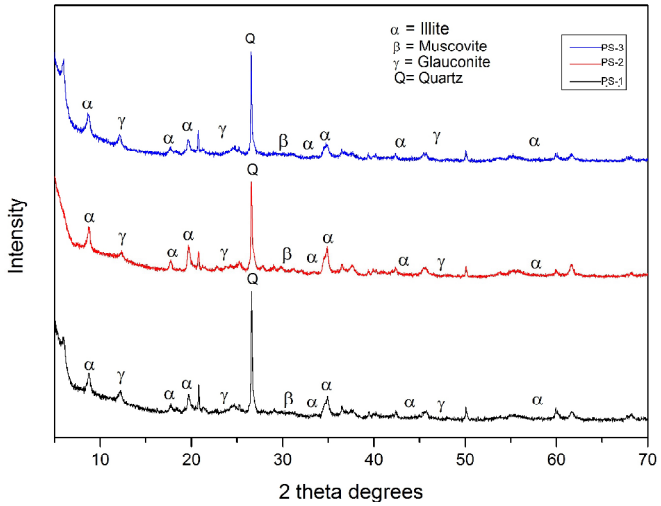

Fig.7. XRD analysis of palaeosol samples named as PS-1, PS-2 and PS-3.

Table 5. CIA, CIW, Palaeo-temperature, Salinization, Clayness of samples calculated from XRF analysis

Sample No.	CIA	CIW	Clayeyness	Salinization	Paleotemperature (°C)
PS-1/1	80.469	98.723	0.127	0.230	13.049
PS-1/2	83.367	97.884	0.076	0.178	14.009
PS-1/3	81.922	98.357	0.071	0.204	13.527
PS-2	75.220	95.961	0.291	0.287	11.984
PS-3	75.345	99.004	0.319	0.317	11.432
PS-4	76.123	95.591	0.289	0.273	12.259

Salt dynamics are among the sensitive indicators for climate change and soil salinization where salinization is basically the molar ratio of K and Na to Al (Retallack, 1997). Since a threshold of 1 is set by Retallack (2001) for significant salinization, here the values are fairly < 1 indicating ratio of Na^+ and K^+ to Al is lower. The clayeyness (Al_2O_3/SiO_2) varies from 0.1 to 0.5 in accordance with salinization which suggests the chemical weathering was not dominant during the deposition.

The Temperature has been calculated (Table-5) to be approximately 11°-14°C which indicates cold climate in which physical weathering dominates over chemical weathering, which is also supported by the CIA value.

CONCLUSION

The presence of the weakly-developed, sandstone hosted, thin palaeosol horizon along the eastern margin of the Pranhita-Godavari valley suggests fluvially influenced shallow marine environment. It

was supported by the presence of clay minerals like glauconite and illite. Although, local sea level fluctuations and exposure of fan-delta sequence for pedogenesis took place for a short duration.

The thin-section studies of palaeosol and sandstone indicate weakly developed pedofeatures in the upper part of the horizon and crude laminations in the lower (primary depositional feature). Limited vertical and horizontal exposure may be attributed to the duration of weathering. The CIA value and presence of clay minerals like illite attest the colder climate ranging between 11-14°C. Less accumulation of and abundance of cations indicate dominance of physical weathering over chemical. However, slight increase of Al_2O_3 in middle part of profile attributed to thin clay accumulation zone as generally found in all soil profiles.

References

Abbott, P.L., Minch, J.A. and Peterson, G.L. (1976) Pre-Eocene paleosol south of Tijuana, Baja California, Mexico. Jour. Sediment. Res., v.46(2), pp.355-361.

Amarasinghe, U., Chaudhuri, A., Collins, A.S., Deb, G., Patranabis-Deb, S., (2015) Evolving provenance in the Proterozoic Pranhita-Godavari Basin, India. Geoscience Frontiers, v.6(3), pp.453–463.

Amorosi, A. (1997) Detecting compositional, spatial, and temporal attributes of glaucony: a tool for provenance research. Sedimentary Geol., v.109(1-2), pp.135-153.

Arndorff, L. (1993) Lateral relations of deltaic palaeosols from the Lower Jurassic Rønne Formation on the island of Bornholm, Denmark. Palaeogeo., Palaeoclimat., Palaeoeco., v.100(3), pp.235-250.

Birkeland, P.W. (1999) Soils and Geomorphology, (3rd Ed.). Oxford University Press, New York. 448p.

Bhargava, O.N., Kaur, G. and Deb, M. (2011) A Paleoproterozoic paleosol horizon in the Lesser Himalaya and its regional implications. Jour. Asian Earth Sci., v.42(6), pp.1371-1380.

Boggs, S. (2006) Principles of Sedimentology and Stratigraphy, 4th edition. Pearson Prentice Hall, Upper Saddle River, New Jersey. 662p.

Buol, S.W., Hole, F.D., McCracken, R.J., Southard, R.J. (1997) Soil Genesis and Classification (4th edn.), Iowa State University Press, Ames, 527p.

Chaudhuri, A., Howard, J.D. (1985) Ramgundam Sandstone; a middle Proterozoic shoal-bar sequence. Jour. Sediment. Res., v.55(3), pp.392–397.

Chaudhuri, A.K., Saha, D., Deb, G.K., Deb, S.P., Mukherjee, M.K. and Ghosh, G. (2002) The Purana basins of southern cratonic province of India-a case for Mesoproterozoic fossil rifts. Gondwana Res., v.5(1), pp.23-33.

Conrad, J.E., Hein, J.R., Chaudhuri, A.K., Patranabis-Deb, S., Mukhopadhyay, J., Deb, G.K., Beukes, N.J. (2011) Constraints on the development of Proterozoic basins in central India from 40Ar/39Ar analysis of authigenic glauconitic minerals. Geol. Soc. Amer. Bull., v.123(1-2), pp.158–167.

Crookshank, H. (1963) Geology of southern Bastar and Jeypore from the Bailadila to Easternghats. Mem. Geol. Surv. India, v.87, p.149.

Deb, G. (2003) Deformation pattern and evolution of the structures in the Penganga Group, the Pranhita–Godavari Valley, India: probable effects of Greenvillian movement on a Mesoproterozoic basin. Jour. Asian Earth Sci., v.21(6), pp.567–577.

Dora, M.L. and Randive, K.R. (2015) Chloritisation along the Thanewasna Shear Zone, Western Bastar Craton, Central India: Its Genetic Linkage to Cu-Au Mineralisation. Ore Geol. Rev., v.70, pp.151-172.

Driese, S.G., Srinivasan, K., Mora, C.I., Stapor, F.W. (1994) Paleoweathering of Mississippian Monteagle Limestone preceding development of a lower Chesterian transgressive systems tract and sequence boundary, middle Tennessee and northern Alabama. Geol. Soc. Amer. Bull., v.106(7), pp.866–878.

Driese, S.G., Medaris Jr, L.G., Ren, M., Runkel, A.C. and Langford, R.P., (2007) Differentiating pedogenesis from diagenesis in early terrestrial paleoweathering surfaces formed on granitic composition parent materials. Jour. Geol., v.115(4), pp.387-406.

Driese, S.G., Nordt, L.C. (2013) New frontiers in paleopedology and terrestrial paleoclimatology: paleosols and soil surface analog systems: *In:* Driese, S.G., Nordt, L.C. (Eds.), new frontiers in paleopedology and terrestrial paleoclimatology. SEPM, Spec. Publ., no.104, pp.1–3.

Driese, S.G. and Ashley, G.M. (2016) Paleoenvironmental reconstruction of a paleosol catena, the Zinj archeological level, Olduvai Gorge, Tanzania. Quaternary Res., v.85(1), pp.133-146.

Fastovsky, D.E., McSweeney, K. (1987) Paleosols spanning the Cretaceous-Paleogene transition, eastern Montana and western North Dakota. Geol. Soc. Amer. Bull., v.99(1), pp.66–77.

Feakes, C.R. and Retallack, G.J. (1988) Recognition and chemical characterization of fossil soils developed on alluvium; a Late Ordovician example. Geol. Soc. Amer. Spec. Papers, no.216, pp.35-48.

Fedo, C.M., Nesbitt, H.W., Young, G.M. (1995) Unravelling the effects of potassium metasomatism in sedimentary rocks and paleosols, with implications for paleoweathering conditions and provenance. Geology, v.23(10), pp.921–924.

Galan, E. (2006) Genesis of clay minerals. Developments in clay science, 1, pp.1129-1162.

Ghosh, G., Saha, D. (2003) Deformation of the Proterozoic Somanpalli Group, Pranhita-Godavari valley, South India - implication for a Mesoproterozoic basin inversion. Jour. Asian Earth Sci., v.21(6), pp.579–594.

Gray, N.B. and Nickelsen, R.P. (1989) Pedogenic slickensides, indicators of strain and deformation processes in redbed sequences of the Appalachian foreland. Geology, v.17(1), pp.72-75.

Gregory, L.C., Meert, J.G., Bingen, B.A., Pandit, M.K., Torsvik, T.H. (2009) Paleo- magnetism and geochronology of the Malani igneous suite, Northwest India: implications for the configuration of Rodinia and the assembly of Gondwana. Precambrian Res., v.170(1), pp.13–26.

Hamer, J.M.M., Sheldon, N.D., Nichols, G.J., Collinson, M.E. (2007) Late Oligocene–early Miocene palaeosols of distal fluvial systems, Ebro Basin, Spain. Palaeogeo. Palaeoclimat. Palaeoeco., v.247(3), pp.220–235.

Harnois, L. (1988) The CIW index: A new chemical index of weathering. Sediment. Geol., v.55(3-4), pp.319-322.

Holland, H.D. (1984) The chemical evolution of the atmosphere and oceans: Princeton University Press. Princeton University Press, Princeton, New Jersey, 582p.

Holland, H.D., Feakes, C.R., Zbinden, E.A. (1989) The Flin Flon paleosol and the composition of the atmosphere 1.8 BYBP. Amer. Jour. Sci., v.289(4), pp.362–389.

Holland, H.D. (1994) Early Proterozoic atmospheric change. *In:* Bengtson, S. (Ed.), Early Life on Earth: Nobel Symposium No. 84. Columbia University Press, New York.

Johnson, H.D. (1975) Tide-and wave-dominated inshore and shoreline sequences from the late Precambrian, Finnmark, North Norway. Sedimentology, v.22(1), pp.45-74.

Klein, C. and Dutrow, B. (2008) Mineral Science. Hoboken.

Kraus, M. (1999) Paleosols in calstic sedimentary rocks: their geologic applications. Earth Sci. Rev., v.47(1), pp.41–70.

Lander, R.H., Bloch, S., Mehta, S., Atkinson, C.D. (1991) Burial diagenesis of paleosols in the giant Yacheng gas field, People's Republic of China: bearing on illite reaction pathways. Jour. Sediment. Res., v.61(2), pp.256–268.

Li, Y.H. (2000) A Compendium of Geochemistry: from solar nebula to the human brain. Princeton University Press, Princeton, 475p.

Liivamägi, S., Somelar, P., Vircava, I., Mahaney, W.C., Kirs, J. and Kirsimäe, K. (2015) Petrology, mineralogy and geochemical climofunctions of the Neoproterozoic Baltic paleosol. Precambrian Res., v.256, pp.170-188.

Maynard, J.B., 1992. Chemistry of modern soils as a guide to interpreting Precambrian paleosols. Jour. Geol., v.100(3), pp.279–289.

McRae, S.G. (1972) Glauconite. Earth Sci. Rev., v.8(4), pp.397-440.

Mitchell, R.L., Sheldon, N.D. (2009) Weathering and paleosol formation in the 1.1 Gakeweenawan Rift. Precambrian Res., 168(3), pp.271–283.

Mukhopadhyay, J., Crowley, Q.G., Ghosh, S., Ghosh, G., Chakrabarti, K., Misra, B., Heron, K. and Bose, S. (2014) Oxygenation of the Archean atmosphere: New paleosol constraints from eastern India. Geology, v.42(10), pp.923-926.

Munsell (2005) Munsell Soil Colour Charts: Matte Collection. Macbeth Division of Kollmorgen Corp., Baltimore.Nesbitt, H. W. and Young, G.M., 1982. Early Proterozoic climates and plate motions inferred from major element chemistry of lutites. Nature, v.299(5885), pp.715–717.

Nordt, L.C., Driese, S.G. (2012) New weathering index improves paleorainfall estimates from vertisols. Geology, v.38(5), pp.407–410.

Odin, G.S. and Fullagar, P.D. (1988) Chapter C4 geological significance of the glaucony facies. Developments in Sedimentology, 45, pp.295-332.

Odin, G.S. and Matter, A. (1981) De glauconiarum origine. Sedimentology, v.28(5), pp.611-641.

Pati, P. (2010) Large scale geological mapping of Archaean-Proterozoic

boundary zone around Sukwasi, southeast of Heti PGE prospect, Chandrapur district, Maharashtra. Geological Survey of India, Training Institute, (Un Pub.).
Pati, P., Parkash, B., Awasthi, A.K. and Jakhmola, R.P. (2012) Spatial and temporal distribution of inland fans/terminal fans between the Ghaghara and Kosi rivers indicate eastward shift of neotectonic activities along the Himalayan front. A study from parts of the upper and middle Gangetic plains, India. Earth Sci. Rev., v.115(4), pp.201-216.
Prochnow, S.J., Nordt, L.C., Atchley, S.C., Hudec, M.R. (2006) Multi-proxy paleosol evidence for middle and late Triassic climate trends in eastern Utah. Palaeogeo. Palaeoclimat. Palaeoeco., v.232(1), pp.53–72.
Prothero, D.R. and Schwab, F. (2004) Sedimentary Geology. Macmillan.
Retallack, G.J., Grandstaff, D., Kimberley, M. (1984) The promise and problems of Precambrian paleosols. Episodes, v.7(2), pp.8–12.
Retallack, G.J. (1986) Reappraisal of a 2200 Ma-old paleosol near Waterval Onder, South Africa. Precambrian Res., v.32(2-3), pp.195–232.
Retallack, G.J. (1988) Field recognition of Paleosols. Geol. Soc. Amer. Spec. Paper, 216, pp.1-20
Retallack, G.J. (1992) How to find a Precambrian paleosol. In Early Organic Evolution (pp. 16-30). Springer Berlin Heidelberg.
Retallack, G. (1997) A Colour Guide to Paleosols. JohnWiley and Sons, New York.
Retallack, G.J. (2000) Depth to pedogenic carbonate horizon as a paleo-precipitation indicator? comment and reply comment. Geology, v.28(6), pp.572–573.
Retallack, G.J. (2001) Cenozoic expansion of grasslands and climatic cooling. Jour. Geol., v.109(4), pp.407–426.
Retallack, G.J. (2013) Ediacaran life on land. Nature, v.493(7430), p.89.
Ruxton, B.P. (1968) Measures of the degree of chemical weathering of rocks. Jour. Geol., v.76(5), pp.518-527.
Singh, S., Awasthi, A.K., Parkash, B. and Kumar, S. (2013) Tectonics or climate: What drove the Miocene global expansion of C4 grasslands? Internat. Jour. Earth Sci., v.102(7), pp.2019-2031.
Singh, S., Parkash, B. and Awasthi, A.K. (2015) Tectono-geomorphic and environmental set-up deduced during deposition of Mio-Pleistocene sediments in NW Himalaya, India. Catena, v.126, pp.173-188.
Singh, S., Ghosh, P. and Khanna, Y. (2017) Need for re-apprehension of basin tectono-depositional set-up during initial stage of Himalayan orogeny from pedogenic evidences. Catena, v.156, pp.102-112.
Sheldon, N.D., Retallack, G.J., Tanaka, S. (2002) Geochemical Climofunctions from North American Soils and Application to Paleosols across the Eocene-Oligocene Boundary in Oregon. Jour. Geol., v.110(6), pp.687–696.
Sheldon, N.D. (2003) Pedogenesis and geochemical alteration of the picture gorge subgroup, Columbia River Basalt, Oregon. Geol. Soc. Amer. Bull., v.115(11), pp.1377–1387.
Sheldon, N.D. (2006) Precambrian paleosols and atmospheric CO2 levels. Precambrian Res., v.147(1), pp.148–155.
Sheldon, N.D., Tabor, N.J. (2009) Quantitative paleoenvironmental and paleoclimatic reconstruction using paleosols. Earth Sci. Rev., v.95(1), pp.1–52.
Soreghan, G.S., Elmore, R.D., Katz, B., Cogoini, M., Banerjee, S. (1997) Pedogenically enhanced magnetic susceptibility variations preserved in Paleozoic loessite. Geology, v.25(11), pp.1003–1006.
Tandon, S.K., Sood, A., Andrews, J.E., Dennis, P.F. (1995) Palaeoenvironments of the dinosaur-bearing Lameta Beds (Maastrichian), Narmada valley, central India. Palaeogeo. Palaeoclimat. Palaeoeco., v.117(3-4), pp.153–184.
Tandon, S.K. and Gibling, M.R. (1997) Calcretes at sequence boundaries in Upper Carboniferous cyclothems of the Sydney Basin, Atlantic Canada. Sediment. Geol., v.112(1-2), pp.43-67.
Torsvik,T.H., Carter, L.M.,Ashwal, L.D., Bhushan, S.K., Pandit, M.K., Jamtveit, B. (2001) Rodinia refined or obscured: palaeomagnetism of the Malani igneous suite(NW India). Precambrian Res., v.108(3), pp.319–333.
Valdiya, K.S. (2010) The making of India: Geodynamic Evolution.Macmillan Publishers India Ltd, New Delhi, 816p.
Varela, A.N., Raigemborn, M.S., Richiano, S., White, T., Poiré, D.G. and Lizzoli, S. (2017) Late Cretaceous paleosols as paleoclimate proxies of high-latitude Southern Hemisphere: Mata Amarilla Formation, Patagonia, Argentina. Sediment. Geol., v.363, pp.83-95.
Weaver, C.E. (1956) A Discussion on the Origin of Clay Minerals in Sedimentary Rocks. Clays and Clay Minerals, v.5, pp.159-173.
Weaver, C.E. (1968) Relations of composition to structure of dioctahedral 2: 1 clay minerals. Clays and Clay Minerals, v.16, pp.51-61.
Webb, G.E. (1994) Paleokarst, paleosol, and rocky-shore deposits at the Mississippian- Pennsylvanian unconformity, northwestern Arkansas. Geol. Soc. Amer. Bull., v.106(5), pp.634–648.
Wright, V.P., 1994. Paleosols in shallow marine carbonate sequences. Earth-Science Reviews, 35(4), pp.367–395.
Wright, V.P., Platt, N.H. (1995) Seasonal wetland carbonate sequences and dynamic catenas: a re-appraisal of palustrine limestones. Sediment. Geol., v.99(2), pp.65–71.
Young, G.M. and Nesbitt, H.W. (1998) Processes controlling the distribution of Ti and Al in weathering profiles, siliciclastic sediments and sedimentary rocks. Jour. Sediment. Res., v.68(3), pp.448-455.
Zbinden, E.A., Holland, H.D., Feakes, C.R., Dobos, S.K. (1988) The Sturgeon Falls paleosol and the composition of the atmosphere 1.1Ga BP. Precambrian Res., v.42(1-2), pp.141–163.

(Received: 8 November 2017; Revised form accepted: 1 January 2018)

Appendix

PS-1
JCPDS # 00-026-0911
Type of illite found is 2M1, monoclinic system
d-spacing of those peak which show 2M1 polytypes are: 3.34 Å, 10 Å
JCPDS # 00-043-0685
Type of illite found is 2M2, monoclinic
d-spacing of the peaks showing 2M2 polytypes are: 4.49Å, 3.34Å

PS-2
JCPDS # 00-009-0911
Type of illite found is 2M1, monoclinic system
d-spacing of those peak which show 2M1 polytypes are: 3.34 Å, 10 Å
JCPDS # 00-043-0685
Type of illite found is 2M2, monoclinic system
d-spacing of those peak which show 2M2 polytypes are: 5.06 Å, 4.49 Å, 3.34Å, 2.58Å, 2.51Å
JCPDS # 00-024-0495
Type of illite found is 2M2, monoclinic system
d-spacing of those peak which show 2M2 polytypes are: 2.58Å, 2.51Å, 2.46Å

PS-3
JCPDS # 00-009-0911
Type of illite found is 2M1, monoclinic system
d-spacing of those peak which show 2M1 polytypes are: 10Å, 4.48Å, 3.33Å,2.56Å, 2.50Å
JCPDS # 00-009-0334
Type of illite found is 2M1, monoclinic system
d-spacing of those peak which show 2M1 polytypes are: 10Å,1.29Å, 1.5Å
JCPDS # 00-024-0495
Type of illite found is 2M1, monoclinic system
d-spacing of those peak which show 2M1 polytypes are: 4.48Å,2.51Å, 2.45Å, 2.28Å